This article has been accepted for publication in a future issue of this journal, but has not been fully edited. Content may change prior to final publication. Citation information: DOI 10.1109/JRFID.2022.3154630, IEEE Journal of Radio Frequency Identification

Design and Experimental Characterization of On-skin Loop Antenna for Next 5G Backscattering-based Communications

C. Occhiuzzi*, F. R. Venturi*, F. Amato$, A. Di Carlofelice†, P. Tognolatti†, G. Marrocco*

***Abstract*—Backscattering-based communications are promising solutions for large scale body-centric monitoring systems, for the low power requirements and the simple and lightweight electronics. Currently, UHF frequency band represents the golden standard, mainly thanks to the well assessed Radio Frequency IDentification (RFID) technology. However, early studies proposed the exploitation to the upcoming 5G communication infrastructures to overcome the limitations in bit-rate and bandwidth and the need of a dedicated reading platform to interact with the tags. The aim of the work is to experimentally verify, from the antenna perspective, the possibility to adopt the 5G 3.6 GHz frequency band also for the next generation body-centric backscattering systems. An epidermal loop antenna is hence designed and prototyped. Measurements in real conditions, e.g. on the human body and through a custom testbed emulating a real backscattering link, are presented as well as statistical analysis on human variability. Results over five volunteers confirm the possibility to read the epidermal tag up to 1.2 m, hence enabling monitoring within a medium-size room.**

***Index Terms*—backscattering communications, epidermal electronics, body-centric systems, 5G**

I. Introduction

IN the framework of Internet of Things (IoT), *Healthcare* (H)-IoT [1] is becoming a particularly attractive opportunity. Nowadays, a network of body-worn devices and sensors can connect ourselves with the external world seamlessly and continuously gathering information about our health and activity. Biophysical data can be directly collected on the skin [2] through devices capable to sample the human sweat to retrieve pH, lactate, electrolytes and cortisol or by performing temperature, breath, ECG and EMG measurements [3]. A critical challenge toward this vision is to design devices that can be easily deployed on the body and run autonomously without impacts on energy supply and costs: battery-less solutions and lightweight and simple electronics appear hence mandatory. Backscatter communication [4], [5] is gaining popularity as a suitable solution to fulfill such a need [6], especially when commodity signals are exploited. Devices based on ambient backscatter communications (ABSCs) [7] can communicate with each other by modulating and reflecting surrounding signals that are broadcasted from ambient RF sources such as WiFi, Bluetooth and Cellular mobile phone, hence improving interoperability and spatial and technological flexibility. Additional opportunities could arise from the exploitation of Orthogonal Frequency-Division Multiplexing (OFDM) 5G communication systems [8], [9]. Several backscattering architectures were recently stimulated by the improved bandwidth [10], by massive multiple input multiple output (M-MIMO) antennas, by beamforming capabilities of the 5G [11], and by the possibility to easily create personal area networks through access points and personal devices [12] communicating over multiple frequencies and services [13]. Although a standard modulation scheme is still missing, early investigation and experiments demonstrated the advantages of the proposed platform in terms of read distance [14], [15], bitrate [16] and coverage [17].

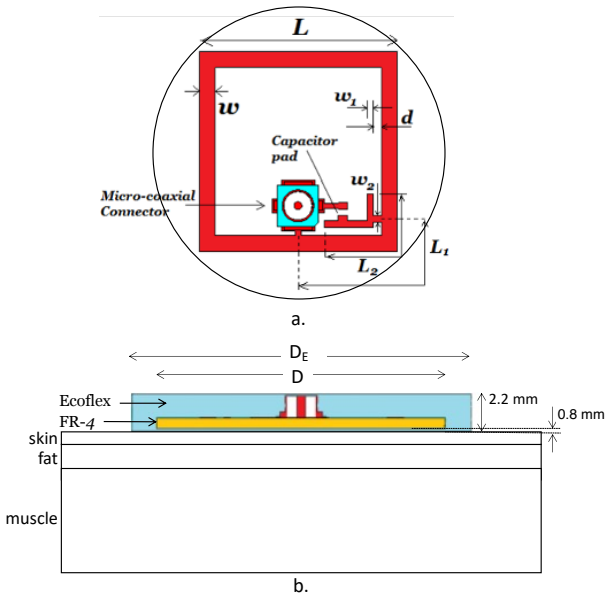

Fig. 1. Layout of the reference Epidermal Loop including the internal gamma-match transformer. Top view (a) and side view (b) with the detail of the shell in Ecoflex and the multilayered phantom simulating the human body. Relative permittivity, electrical conductivity, thickness (Skin 1 mm, εr = 36.92, s = 2.08 S/m - Fat 3 mm, εr = 5.16, s = 0.16 S/m - Muscle 31 mm, εr = 51.32, s = 2.65 S/m).

The potential of using 5G backscattering communication was investigated in [18] also for bodycentric systems, with particular focus to epidermal battery-less sensors. Theoretical

* University of Roma "Tor Vergata", DICII, Via del Politecnico 1, Rome e-mail: cecilia.occhiuzzi@uniroma2.it.

$ ITIS Galileo Galilei, Rome, Italy.

† University of L'Aquila, Dipartimento di Ingegneria industriale e dell'informazione e di economia, Piazzale Ernesto Pontieri, Monteluco di Roio, L'Aquila.

This work was supported by the University of Rome Tor Vergata within " Beyond Borders-Epidermal Sensor Networks for Emerging 5G systems", under Grant E84I19002410005.

This article has been accepted for publication in a future issue of this journal, but has not been fully edited. Content may change prior to final publication. Citation information: DOI 10.1109/JRFID.2022.3154630, IEEE Journal of Radio Frequency Identification

achievable performances were compared with the ones offered by the well assessed epidermal RFID sensor tags operating in the UHF (860-960 MHz) [19] band. In spite of the higher free space attenuation, S-band (3.6 GHz) on-skin antennas would be suitable to provide comparable read distances, while boosting smaller layouts and much higher data rate. Early experimental tests in simplified reference conditions (*i.e.:* over human body phantom and by measuring only S11 and S21 parameters of half antennas over ground plane [20]) demonstrated that, similarly to UHF band, optimal antenna configurations exist also in the S-band and that much better performance could be achieved by using array configurations [21]. However, the numerical outcomes still need to be demonstrated in realistic conditions, namely when a true matched antenna is placed on the skin and a backscattering link is established with a 3.6 GHz radio.

To close the circle, this paper describes an extensive experimental campaign with a reference on-skin antenna aimed at corroborating the above numerical findings. More specifically, a reference $\lambda - loop$ is here designed and prototyped. Like conventional epidermic devices, the antenna is encapsulated into a biocompatible polymer and stacked directly on the skin of different male and female volunteers. Gain and input impedance are measured on several on-body positions and compared with measurements performed over reference phantom to statistically evaluate the effects of human variability. By exploiting a custom setup based on a Software Defined Radio and a modulator, the backscattering reader-tag link at 3.6 GHz is emulated to retrieve the differential radar cross section of the antenna. Measurements are finally used to *i)* corroborate the theoretical expectation in terms of maximum achievable gain, *ii)* evaluate the robustness of the S-band backscattering link against the effects of the human body and finally *iii)* compare the performances with the ones of typical epidermal UHF antennas in terms of expected read distance and antenna footprint.

The paper is organized as follow: the design, the prototype and the test in reference configurations of the epidermal antenna are discussed in Section II. On-body measurements are then described in Section III and discussed in terms of achievable performance in Section IV.

II. Reference 3.6 GHz loop antenna

Without loss of generality, the reference epidermal antenna (Fig. 1a.) comprises a squared $\lambda-$loop of side L and an internal Gamma-match transformer hosting the feeding point. The Gamma-match guarantees a fine control of the input impedance, an improved bandwidth and simultaneously enables the connection to the unbalanced coax cable [25]. A capacitor C in series to the gamma-match strip is finally included to compensate the inductive reactance introduced by the short-circuited transmission line formed by the loop element and the gamma strip. Although flexible substrates would be more suitable to on-skin placement, a $0.6\ mm$ FR4 ($\epsilon_r = 4.3, tan\delta = 0.025$) PCB is here considered for the sake of robustness and the easiness of fabrication and measurements. Similarly, to make the antenna more compliant

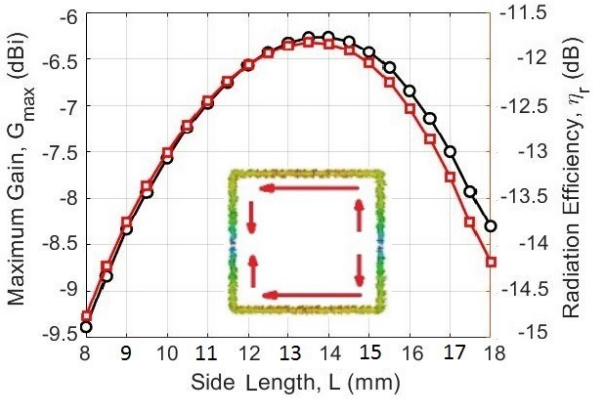

a.

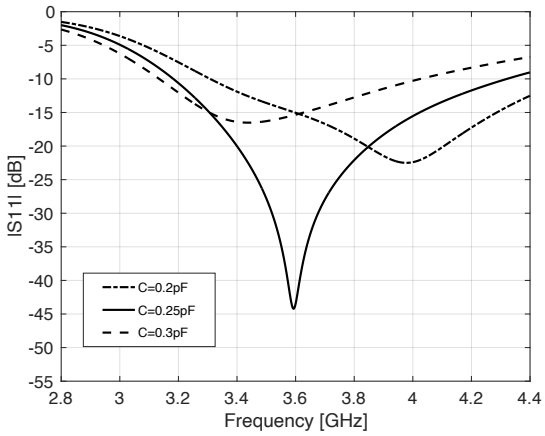

b.

Fig. 2. On-skin square loop. Optimum gain (a) and S11 (b) $\{L, w, L1, L2, w1, d\} = \{13.5, 1, 6.95, 5.21, 0.4, 0.5\}$

with the human body, the FR4 profile is rounded and the prototype is encapsulated within a 2.2 mm thick layer of Ecoflex 00-30 [26], namely a biocompatible silicone rubber-based polymer with adhesive properties whose dielectric parameters $\epsilon_r = 2.8,\ tan\delta = 0.02$ were estimated from [27]. Overall, the loop is placed at a distance of $u = 0.8\ mm$ from the body, as in (Fig. 1b.). The antenna is designed by the help of FDTD simulations (performed with CST Microwave Studio), including an 80x80 mm^2 3-layers body phantom as visible in Fig. 1b.

A. Design

The design of the antenna is accomplished by a two-steps procedure. First, by considering only the external loop, the optimal size of the antenna in terms of gain is identified by acting on the length L of the side. Results are shown in Fig. 2a. An optimum value L_{opt} exists for $L = 13.5$ mm, corresponding to $G_{max} = -6.3$ dBi and a radiation efficiency $\eta = -11.7$ dB$\sim 8\%$. In agreement with typical epidermal loops [19], [28], when $L = L_{opt}$, a symmetric distribution of currents is excited (inset of Fig. 2a.). Two facing sides host in-phase currents that produce radiation and power loss in the body. The other two sides host currents with opposite

This article has been accepted for publication in a future issue of this journal, but has not been fully edited. Content may change prior to final publication. Citation information: DOI 10.1109/JRFID.2022.3154630, IEEE Journal of Radio Frequency Identification

phase and contribute only to the power loss. Nulls are located in the middle of the non-radiating sides leading to a linear horizontal polarization. Optimal values are in agreement with what expected from [18].

For the optimal loop size, the input impedance is then optimized by acting on the Gamma-match strip length $L2$ and on the value C of the SMD capacitor in series with the strip. The former mainly impacts on the real part of the input impedance, the latter instead determines the resonance frequency f (Fig. 2b). Since backscattering microchips are not yet available at 3.6 GHz, the antenna was matched to $Z_L = 50\ \Omega$. By considering $C = 0.25\ pF$ and $L_1 = 6.95\ mm$ (other parameters are listed in the caption of Fig. 2), the resulting input impedance is $Z_{in} = 50.7 - j0.6\ \Omega$ @ 3.6 GHz, corresponding to $|S11| \sim -45\ dB$ and a relative bandwidth $B_{-10dB} \approx 31\%$. It is worth noticing that the capacitance C sensibly affects the resonance frequency of the antenna. Tolerances and uncertainties of real components could hence make necessary post-designing tuning, e.g. by slightly changing the value of the selected discrete capacitor. However, the impedance transformer leads to a large bandwidth, with benefits in compensating typical detuning effects due to human variability [19]. Broadside gain of the final configuration is $G \approx -8$ dBi.

B. Prototype

A prototype of the loop was manufactured through the 4MILL300 ATC milling machine. A SMP connector, a micro-coax cable for connecting to VNA and a Murata GJM1555CHR27BB01 capacitor were integrated on the board. The Ecoflex shell was obtained by pouring the liquid polymer into a plastic mold containing the antenna and the cable. The sample was then stored at ambient temperature for 4 hours to cure the elastomers. Resulting prototype is flat and pretty uniform. The resulting device is visible in Fig. 3.

S11 was measured by a vector network analyzer (MS2024A) when the antenna was attached onto a cubic body phantom (cooked pork with estimated parameters $\epsilon_r = 40$ and σ = 2 S/m [18]). To reduce the impact of the cable, this was passed through the phantom, that therefore acts as an absorber, and then connected to the VNA behind. The antenna required marginal manual tuning to 3.6 GHz by acting on the capacitor $C = 0.4\ pF$ to compensate for uncertainties in realization, components and phantom. A not negligible impact is expected to be given by the coaxial cable who turns right in the middle of the loop. Nevertheless, an acceptable match was obtained (Fig. 4a.), in agreement with the simulations especially in terms of operating frequency. Instead, the measured bandwidth $B_{-10dB} \sim 9\% \approx 32MHz$ is lower respect to the expected one, probably due to the usage of real components, connector and cable. A particular note must be devoted to the equivalent phantom and the uncertainties related to its dielectric properties, especially in terms of losses. Respect to the estimated one, the phantom seems to have a lower conductivity. By considering also the not perfect control in Ecoflex thickness, the reduced measured bandwidth could be hence explained.

Radiation performance was estimated by applying the gain-comparison method [25]. For this purpose, a reference linearly

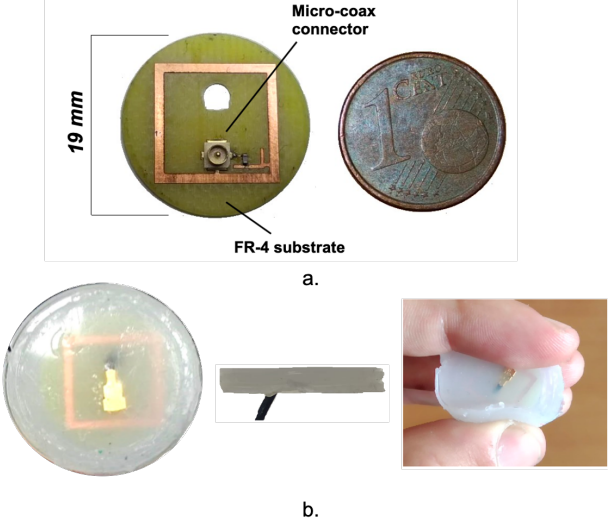

Fig. 3. Prototype of the epidermal loop. a) Bare PCB with the SMA micro connector and the SMD capacitor. The hole is necessary to the insertion of the coaxial cable; b) antenna and coaxial cable embedded within a 2 mm-tick Ecoflex layer. The pouring of the Ecoflex was done on the complete layout, comprising the antenna, the capacitor, the SMP connector and the coaxial cable properly passing through the hole such to be positioned behind the antenna.

TABLE I
DETAILS OF THE VOLUNTEERS

Subject	Sex	Age	Body Mass Index (BMI)
1	M	26	21.95
2	M	24	22.9
3	M	22	17.59
4	F	22	19.96
5	F	22	19.47

polarized folded patch antenna with a central radiating slot (Fig.5) [29] was designed, prototyped and fully characterized in terms of S11 and gain in different configurations (in free space, on ground plane and on the human body phantom). Reference patch was then measured on the same body phantom and in the same geometrical arrangement of the loop under test. As in conventional on-body antennas, due to the reflective features of the human body, radiation pattern (visible in Fig. 4 b) presents a main lobe in the off-body direction. The obtained maximum gain and beamwidth are $G_{max} \sim -7.2$ dBi and $BW_{-3dB} = 105°$, respectively. Results are in agreement with the simulations ($|G_{max-sym} - G_{max-meas}| \approx 1$ dB). Polarization is linear with a co-polar/cross-polar ratio higher than 10 dB in the broadside direction.

III. ON-BODY MEASUREMENTS

The performance of the epidermal loop were evaluated directly on the human body when the antenna was placed on different regions, namely armpit, knee, palm, back of the hand, and elbow (Fig.6). To evaluate the human variability, measurements were carried out on five males and females volunteers, as detailed in Tab. I. A total of 25 measurements were processed.

This article has been accepted for publication in a future issue of this journal, but has not been fully edited. Content may change prior to final publication. Citation information: DOI 10.1109/JRFID.2022.3154630, IEEE Journal of Radio Frequency Identification

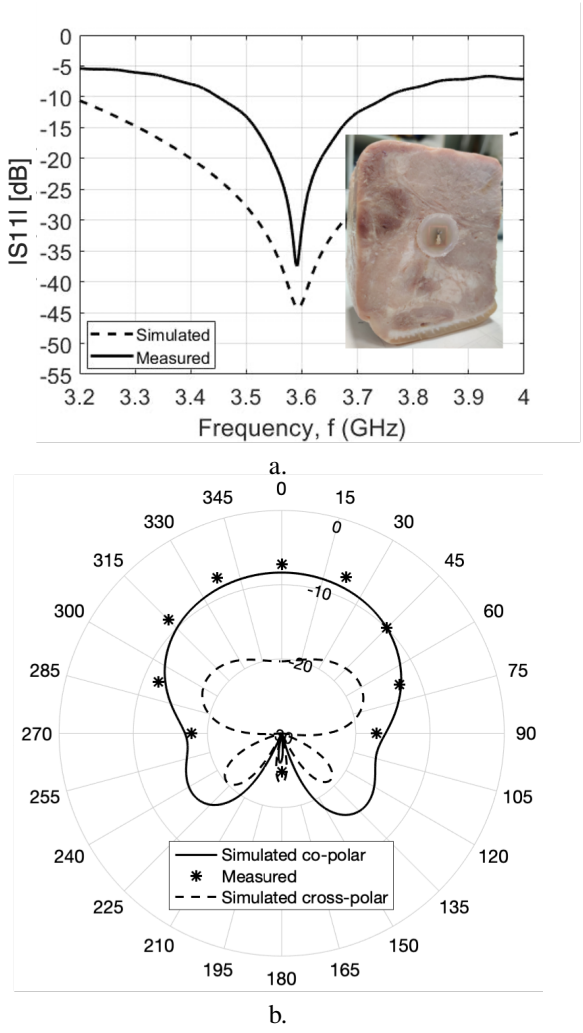

Fig. 4. a) $|S11|$ and b) gain on the $\phi = 0$ plane of the epidermal loop embedded into the Ecoflex measured in semi-anechoic chamber onto a cubic body phantom (inset of a.).

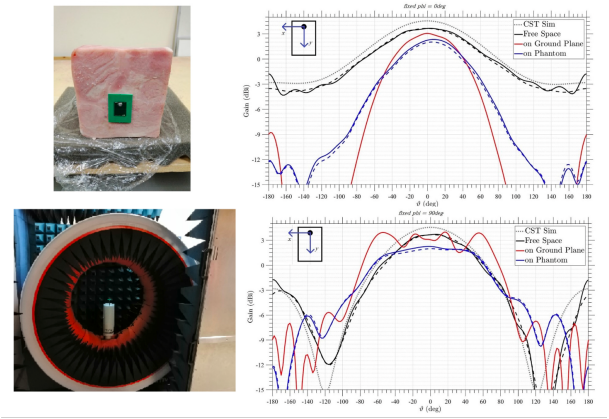

Fig. 5. Measured Gain of the reference patch antenna placed in different configurations. Measurements were conducted through the StarLab 18 in Microwave Vision Italy.

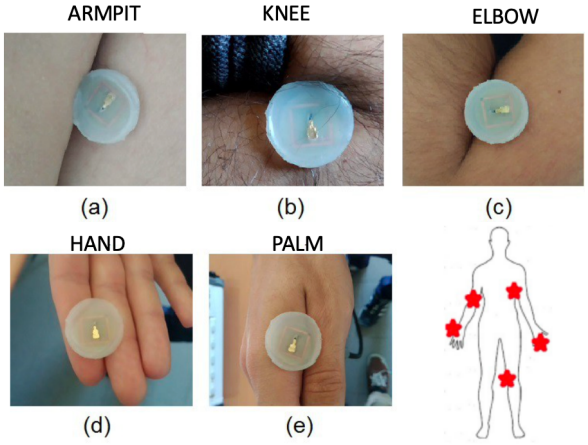

Fig. 6. On-body measurements. For each volunteer five positions on the body were considered .

The S11 was measured in the 3.2-4 GHz band (Fig. 7). To further reduce the impact of the cable, it was passed again through gaps around the arm, leg, and fingers so that it was further shielded by the body and then connected to the VNA behind.

For each position, the body configuration affects the measurements of the five volunteers, with variations in both frequency peak and amplitude. However, results are on average in agreement with the one measured in reference condition. At 3.6 GHz —S11— is lower than -10 dB in every measurement, with an average bandwidth of about 12%. Fig. 8 shows the distribution of the resonance frequency. Generally, with respect to the measurements on the phantom, a slight decrease of the peak is measured, regardless of the position. The mean value and the standard deviation are $3.55\ GHz$ and $0.1\ GHz$, respectively, with a 100% of probability that the peak frequency lays in the $3.3 - 3.8$ GHz 5G S-band range [30].

Similar consideration can be done for the gain, evaluated thorough the comparison method in the broadside direction (results in Fig. 9). As in the UHF band, the anatomical configuration of the different body regions, and the variable physiques (identified by the BMI in Tab. I) produce variations of the maximum achievable values. Except for subject 3, the maximum gain in the broadside direction ranges between -6 and -9 dBi ($G_{avg} = -7.3 \pm 1\ dBi$), in agreement with the measurements on the phantom. The best performances are achieved when the antenna is placed in the armpit region and on the hand. In the former case, it is reasonable to presume an improvement of the antenna directivity since it is backed and surrounded by a large scattering object (human torso and shoulders). In the latter case instead the presence of low lossy tissues underneath the skin (thick corneum layer and bone) produces a better radiation efficiency since losses are reduced.

A. *Radar Cross Section*

The reflected power of the tag in the direction of the receiver can be measured by its radar cross section [16]. In case

This article has been accepted for publication in a future issue of this journal, but has not been fully edited. Content may change prior to final publication. Citation information: DOI 10.1109/JRFID.2022.3154630, IEEE Journal of Radio Frequency Identification

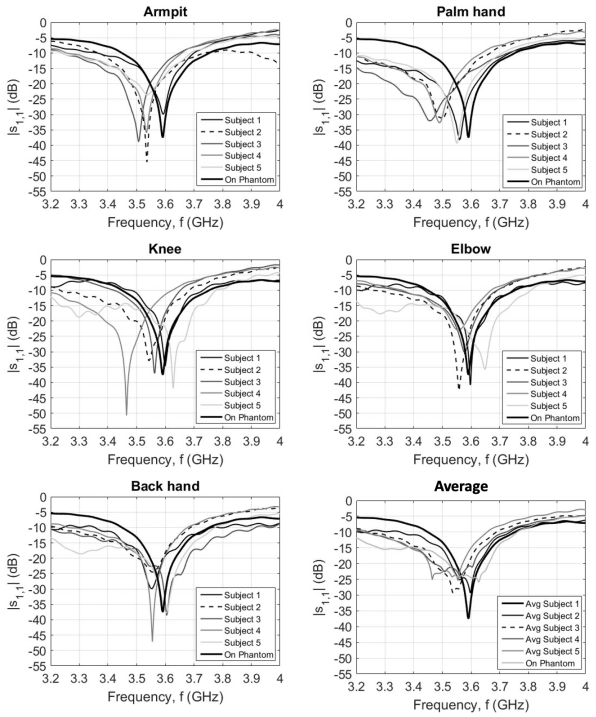

Fig. 7. Measurements of the S11 epidermal loop on the body of the five volunteers and for different body positions.

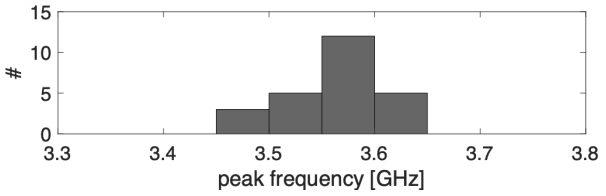

Fig. 8. Distribution of the peak frequency of the reference loop when placed onto different body positions of 5 volunteers.

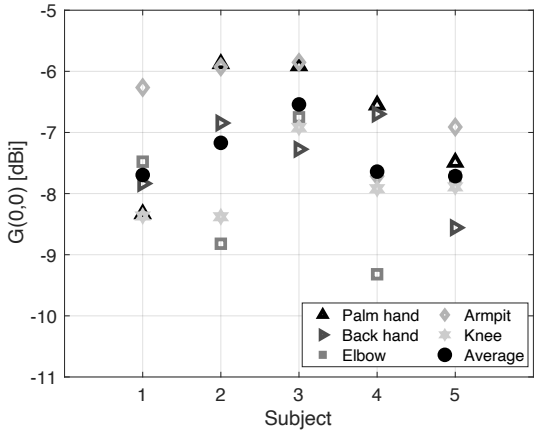

Fig. 9. Measurements of the broadside gain G(0,0) of the epidermal loop on the body. For each subject, dark circle indicates the average value.

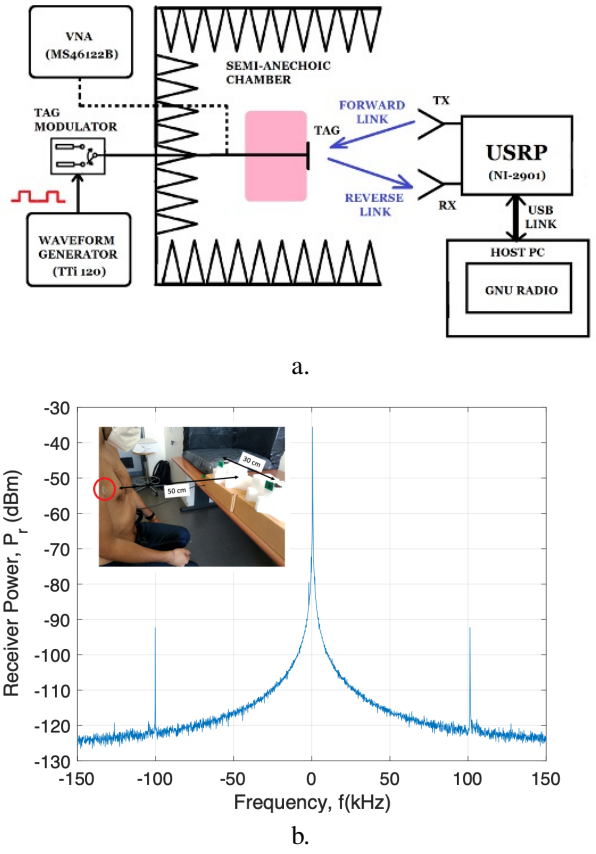

Fig. 10. Measurement setup for the Δrcs. A Universal Software Radio Peripheral interrogates in bi-static configuration the epidermal loop worn by the volunteer. a) Scheme, b) example of the received spectrum. Setup in the inset.

of backscattering through modulated impedance, scattering is related to the difference among the signals reflected back in the different impedances states. The *differential* radar cross section is $\Delta rcs = \frac{\lambda^2 G_T^2}{\pi} M$, with G_T the gain of the antenna and $M = 0.25 \mid \Gamma_{match} - \Gamma_{un-matched} \mid^2$ the load modulation index related to the reflection coefficients Γ in the matched and un-matched state, respectively. The higher the difference between the modulation states, the higher the scattered power is, but the lower the power transferred to the load.

By following the measurement method in [31] that considers the backscattering antenna under test and an illuminating reader, Δrcs can be retrieved by using classical radar equation as:

$$\Delta rcs = \frac{P_r}{P_t G_R^2} \frac{(4\pi)^3 d^4}{\lambda^2} \tag{1}$$

with P_r the power of the received modulated backscattered signal, P_t the power entering in the reader transmitting antenna, G_R the gain of the reader transmit/receive antennas, and d the distance to the tag.

Since dedicated RFID readers and microchip transponders are not available for 3.6 GHz RFIDs yet, a custom testbed operating in the S-band was exploited [29], whose functional scheme is visible in Fig. 10a. The setup consists of two modules: a reader system based on Universal Software Radio Pe-

This article has been accepted for publication in a future issue of this journal, but has not been fully edited. Content may change prior to final publication. Citation information: DOI 10.1109/JRFID.2022.3154630, IEEE Journal of Radio Frequency Identification

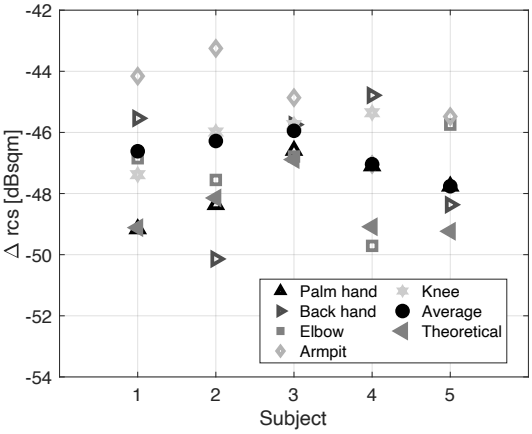

Fig. 11. Measurements of the Δrcs of the epidermal loop on the human body. For each subject, dark circle indicates the average value while filled gray triangle indicates the theoretical value evaluated from the measured gain.

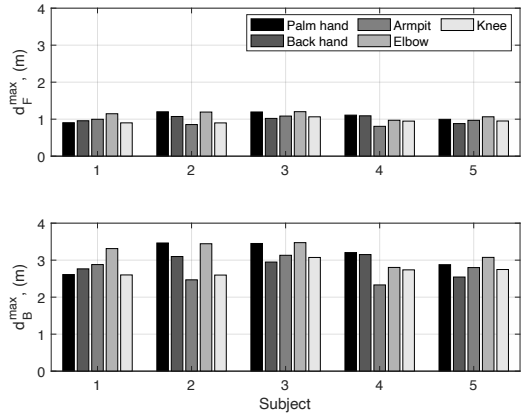

Fig. 12. Estimated read distances of epidermal loop placed on the human body. Direct a) and reverse b) links are evaluated starting from the maximum gain and rcs measured on different volunteers.

ripheral (USRP) NI2901 by Ettus Research™, and a two-state impedance modulator to be connected to the tag antenna. The reader has a bi-static configuration and generates a continuous wave (CW) at carrier frequency $f_c = 3.6\ GHz$; it transmits $P_t G_R = 2mW$. Both receiving and transmitting reference antennas are the folded patches previously described in Section II. The modulator switches between $Z_{match} = 46.5 + j19\ \Omega$ and $Z_{un-matched} = 300 - j259\ \Omega$, with the modulation index $M = 0.2$ and a switching frequency $f_m = 100\ kHz$. Receiving and transmitting reader antennas were placed at a distance $d = 50\ cm$ from the body (Inset of Fig. 10b.). The RF spectrum of the backscattered signal consists of the carrier frequency f_c and the modulated components centered at $f_c \pm f_m$ (Fig. **10**b). After down-converting the signal and filtering out f_c with a DC-block, the amplitudes of the in-phase (I) and quadrature (Q) components of the signal are used to measure the received power level P_r, upon calibration:

$$P_r = \frac{I^2 + Q^2}{Z_0}, \tag{2}$$

with Z_0 being the input impedance of the receiving antenna (Z_0 = 50 Ω); the Δ_{rcs} is then computed using (1).

The measured Δrcs in the different body positions, and for the different subjects, are reported in Fig. 11. As for the gain, the higher values are achieved when the tag is placed in the armpit region, while the lower ones are for hands and elbow. The scattering contribution of the body is hence evident. Despite the human variability, Δrcs is quite stable in the considered band, on average around $-47\ dBsqm$, and in agreement with the expected theoretical results evaluated from the previously measured gains.

IV. Performances analysis

Being the communication completely passive, *i.e.:* based on the backscattering of the impinging waves, communication link is generally limited and subjected to several degrading effects. The two-ways link can be described by the Friis and radar formulas [24]. Denoting with p_t and p_r the transponder and reader sensitivities, respectively, the maximum read distance is the minimum between the maximum forward link range d_F^{max}, and the maximum backward link range, d_B^{max} [24]:

$$d^{max} = min \begin{cases} d_F^{max} = \frac{\lambda}{4\pi} \sqrt{\frac{P_t G_R G_T \tau_T \eta_p}{p_t}} \\ d_B^{max} = \sqrt[4]{\frac{\lambda^2}{4\pi^3} \frac{P_t G_R^2 \Delta rcs \eta_p^2}{p_r}} \end{cases} \tag{3}$$

where η_p is the polarization mismatch between reader and tag antennas and $\tau_T = (4R_{match}R_{loop}) / |Z_{match} + Z_{loop}|^2$ is the power transfer coefficients at the ports of the loop antenna, respectively. Since 5G-oriented electronics for backscattering radios are not yet available, it will be hereafter assumed that the sensitivities of current state-of-the-art UHF-RFID components ($p_t = -15$ dBm [32] and $p_r = -82$ dBm [33], [34]) could be achieved in the future 5G bands and with the maximum power allowed from the reader $P_t G_R = 36$ dBm.

The forward and backward link ranges, based on the previous on-body measurements, are summarized in Fig. 12. The forward read distances span within a $0.8 - 1.2\ m$ range depending on the body parts and the subjects. Due to the power required to activate the IC, backward link is more than $2\ m$ higher than the forward one hence, as in the UHF band, the communication bottleneck remains the forward link [16], unless battery assisted configurations are considered.

Results for all body parts of all users are summarized through the Complementary Cumulative Distribution Functions (CCDFs) that give the probabilities to achieve a given value of read distance regardless the position and the subject. Fig. 13 suggests that these tags can be read, with a probability of 70%, from a distance of nearly one meter.

Finally, it is worth noticing that the estimated read distances, even the smallest ones (80 cm), can be considered compliant with the exposure limits, as computed in [18]. For a reader emitting 36 dBm through a patch antenna placed 20 cm far from the body, the computed average Specific Absorption Rate (SAR) in 1g of tissue is well below $0.5W/kg$, with a peak at the eyes level, in correspondence of the aqueous humor and a sharp attenuation in the first 10 mm of tissue. Such values

This article has been accepted for publication in a future issue of this journal, but has not been fully edited. Content may change prior to final publication. Citation information: DOI 10.1109/JRFID.2022.3154630, IEEE Journal of Radio Frequency Identification

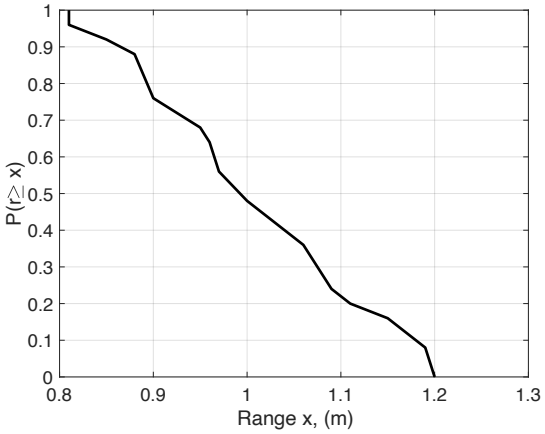

Fig. 13. Complementary Cumulative Distribution Functions (CCDFs) of the maximum read distances of the epidermal sensor on five volunteers.

TABLE II
UHF *vs* S-BAND COMPARISON

Band	Footprint $[mm^2]$	Radiation efficiency	Δf_0	d_{max} [m]	Δd
UHF	900 [19]	3%-6% [28], [35]	7% [19]	1.7 [19] [36]	65% [36]
S-band	300	8%	2%	1.2	35%

must be compared with the FCC conservative restriction of $1.6W/kg$ averaged over 1g.

V. CONCLUSIONS

Extensive experimental characterization of a reference on-skin loop definitively confirmed the numerically foreseen performance of epidermal backscattering communication in the sub-6 GHz 5G band.

A detailed comparison with UHF epidermal antenna is visible in Tab. II. Optimal antenna footprint is almost a tird of the one in UHF band for loops placed $0.1 - 0.5\ mm$ far from the body , while the radiation efficiency is higher. In the S-band, the antenna is more robust against inter/intra human variability for both input impedance and gain. In comparison with the UHF band, the impact of the human body is less effective. Indeed, the spread of the resonance frequency over the considered body position is less than 2%, confirming the positive shielding effect of the human body at higher frequencies.

By considering the electronics constraints of both typical UHF ICs and readers valid, similar read distances are expected. Distances are compliant with the monitoring in a small room or with an on-the-fly acquisition through door gates. In spite of the small size $(A_p \sim 300\ mm^2)$, the best achievable read distance $(d = 1.2\ m)$ is fully comparable with that of a three-times larger UHF antenna. Inter-user variability of read distance is half that of the UHF antenna in comparable arrangement so that retuning mechanisms [19], [36] are not mandatory in the S-band.

REFERENCES

[1] H. Habibzadeh, K. Dinesh, O. Rajabi Shishvan, A. Boggio-Dandry, G. Sharma, and T. Soyata, "A survey of healthcare internet of things (hiot): A clinical perspective," IEEE Internet of Things Journal, vol. 7, no. 1, pp. 53–71, 2020

[2] D.-H. Kim et al., "Epidermal electronics," Science, vol. 333, no. 6044, pp. 838–843, Aug. 2011.

[3] S. Amendola, et al. "More than wearable: Epidermal antennas for tracking and sensing." Electromagnetics of Body Area Networks: Antennas, Propagation, and RF Systems (2016): 319.

[4] C. Xu, L. Yang, and P. Zhang. "Practical backscatter communication systems for battery-free Internet of Things: A tutorial and survey of recent research." IEEE Signal Processing Magazine 35.5 (2018): 16-27.

[5] R. Torres et al., "Backscatter Communications," in IEEE Journal of Microwaves, vol. 1, no. 4, pp. 864-878, Fall 2021, doi: 10.1109/JMW.2021.3110058.

[6] P. Zhang, et al. "Enabling practical backscatter communication for on-body sensors." Proceedings of the 2016 ACM SIGCOMM Conference. 2016.

[7] G. Wang, F. Gao, R. Fan, & C. Tellambura (2016). Ambient backscatter communication systems: Detection and performance analysis. IEEE Transactions on Communications, 64(11), 4836-4846.

[8] Q. Liu, S. Sun, X. Yuan, et al. Ambient backscatter communication-based smart 5G IoT network. J Wireless Com Network 2021, 34 (2021). https://doi.org/10.1186/s13638-021-01917-3

[9] R. Correia and N. B. Carvalho, "OFDM-like High Order Backscatter Modulation," 2018 IEEE MTT-S International Microwave Workshop Series on 5G Hardware and System Technologies (IMWS-5G), Dublin, Ireland, 2018, pp. 1-3. doi: 10.1109/IMWS-5G.2018.8484348

[10] J. Kimionis, A. Georgiadis and M. M. Tentzeris, "Millimeter-wave backscatter: A quantum leap for gigabit communication, RF sensing, and wearables," 2017 IEEE MTT-S International Microwave Symposium (IMS), Honolulu, HI, USA, 2017, pp. 812-815. doi: 10.1109/MWSYM.2017.8058702

[11] Y. Kokar et al., "First Experimental Ambient Backscatter Communication Using a Compact Reconfigurable Tag Antenna," 2019 IEEE Globecom Workshops (GC Wkshps), 2019, pp. 1-6, doi: 10.1109/GCWkshps45667.2019.9024698.

[12] R. Fara, D. Phan-Huy and M. D. Renzo, "Ambient backscatters-friendly 5G networks: creating hot spots for tags and good spots for readers," 2020 IEEE Wireless Communications and Networking Conference (WCNC), Seoul, Korea (South), 2020, pp. 1-7. doi: 10.1109/WCNC45663.2020.9120781

[13] X. Lu, V. Petrov, D. Moltchanov, S. Andreev, T. Mahmoodi and M. Dohler, "5G-U: Conceptualizing Integrated Utilization of Licensed and Unlicensed Spectrum for Future IoT," in IEEE Communications Magazine, vol. 57, no. 7, pp. 92-98, July 2019, doi: 10.1109/MCOM.2019.1800663.

[14] N. Samat, A. Vena, B. Sorli, and J. Podlecki, "Backscattered communication in the 5G band for ultra-low power sensors", in proceedings of URSI France JS20.

[15] J. G. D. Hester and M. M. Tentzeris, "A Mm-wave ultra-long-range energy-autonomous printed RFID-enabled van-atta wireless sensor: At the crossroads of 5G and IoT," 2017 IEEE MTT-S International Microwave Symposium (IMS), 2017, pp. 1557-1560, doi: 10.1109/MWSYM.2017.8058927.

[16] P. Pursula, et al. "Millimeter-wave identification—A new short-range radio system for low-power high data-rate applications." IEEE Transactions on Microwave theory and techniques 56.10 (2008): 2221-2228.

[17] B. Ritayan, and J. Lempiäinen. "Assessment of 5G as an ambient signal for outdoor backscattering communications." Wireless Networks (2021): 1-12.

[18] F. Amato, C. Occhiuzzi, and G. Marrocco, "Epidermal backscattering antennas in the 5G framework: Performance and perspectives," IEEE J. Radio Freq. Identif., vol. 4, no. 3, pp. 176–185, Sep. 2020.

[19] C. Miozzi, S. Nappi, S. Amendola, C. Occhiuzzi, & G. Marrocco, "A general-purpose configurable RFID epidermal board with a two-way discrete impedance tuning". IEEE Antennas and Wireless Propagation Letters, 18(4), 684-687, 2019

[20] F. Amato, C. Occhiuzzi and G. Marrocco, "Performances of a 3.6 GHz Epidermal Loop for Future 5G-RFID Communications," 2020 14th European Conference on Antennas and Propagation (EuCAP), 2020, pp. 1-2, doi: 10.23919/EuCAP48036.2020.9135207.

[21] J. D. Hughes, C. Occhiuzzi, J. Batchelor and G. Marrocco, "Twin-Grid Array as 3.6 GHz Epidermal Antenna for Potential Backscattering 5G Communication," in IEEE Antennas and Wireless Propagation Letters, vol. 19, no. 12, pp. 2092-2096, Dec. 2020, doi: 10.1109/LAWP.2020.3023291.

[22] S. Bouaziz, F. Chebila, A. Traille, P. Pons, H. Aubert, and M. M. Tentzeris, “Novel microfluidic structures for wireless passive temperature telemetry medical systems using radar interrogation techniques in Ka-band,” IEEE Antennas Wireless Propag. Lett., vol. 11, no. 1, pp. 1706–1709, 2012.
[23] S. Dey, J. K. Saha and N. C. Karmakar, "Smart Sensing: Chipless RFID Solutions for the Internet of Everything," in IEEE Microwave Magazine, vol. 16, no. 10, pp. 26-39, Nov. 2015, doi: 10.1109/MMM.2015.2465711.
[24] D. Dobkin, The RF in RFID, 4th ed. Burlington, MA, USA: Elsevier, 2012.
[25] C. A. Balanis, Antenna Theory: Analysis and Design. Hoboken, NJ, USA: Wiley, 2016.
[26] Ecoflex 00-30 https://www.smooth- on.com/products/ecoflex-00-30/
[27] Eom, S.; Lim, S. Stretchable Complementary Split Ring Resonator (CSRR)-Based Radio Frequency (RF) Sensor for Strain Direction and Level Detection. Sensors 2016, 16, 1667. https://doi.org/10.3390/s16101667
[28] C. Occhiuzzi, S. Parrella, F. Camera, S. Nappi and G. Marrocco, "RFID-Based Dual-Chip Epidermal Sensing Platform for Human Skin Monitoring," in IEEE Sensors Journal, vol. 21, no. 4, pp. 5359-5367, 15 Feb.15, 2021, doi: 10.1109/JSEN.2020.3031664.
[29] F. Amato, et al. "S-band testbed for 5G epidermal RFIDs." 2020 XXXIIIrd General Assembly and Scientific Symposium of the International Union of Radio Science. IEEE, 2020. APA
[30] Global update on spectrum for 4G & 5G. Dec.2020 https://www.qualcomm.com/media/documents/files/spectrum-for-4g-and-5g.pdf
[31] P. V. Nikitin, K. V. S. Rao, and R. D. Martinez. "Differential RCS of RFID tag." Electronics Letters 43.8 (2007): 431-432.
[32] Axzon. Accessed: May 29, 2020. [Online]. Available: https://axzon.com/rfm3300-d-magnus-s3-m3d-passive-sensor-ic/
[33] Zebra FX7500. Accessed: May 29, 2020. [Online]. Available: www.zebra.com/gb/en/products/spec-sheets/rfid/rfid-readers/fx7500.html
[34] Impinj Indy RS2000. Accessed: May 29, 2020. [Online]. Available: support.impinj.com/hc/en-us/articles/204969718-Indy-RS2000-Datasheet
[35] S. Amendola and G. Marrocco, "Optimal Performance of Epidermal Antennas for UHF Radio Frequency Identification and Sensing," in IEEE Transactions on Antennas and Propagation, vol. 65, no. 2, pp. 473-481, Feb. 2017, doi: 10.1109/TAP.2016.2639829.
[36] S. Amendola, S. Milici and G. Marrocco, "Performance of Epidermal RFID Dual-loop Tag and On-Skin Retuning," in IEEE Transactions on Antennas and Propagation, vol. 63, no. 8, pp. 3672-3680, Aug. 2015, doi: 10.1109/TAP.2015.2441211.

Cecilia Occhiuzzi (Member, IEEE) is Associate Professor at the University of Roma Tor Vergata, where she teaches electromagnetic fields and Biomedical Interaction. She is also Co-Founder and CEO of RADIO6ENSE, a spin-off of the same University active in RFID solutions for the industrial sector. Her research interests include wireless health monitoring by means of wearable and implantable radiofrequency/mm-wave identification techniques and pervasive sensing paradigms for food sector and Industry 4.0.

Francesco R. Venturi is born in Rome in 1995. He graduated in Electronic Engineering at the University of Roma Tor Vergata (Italy). In 2021 he was a research fellow in the same university. His main scientific interests were RFID applications in the 5G band, design of antennas and software defined radio.

Francesco Amato received his B.S. and M.S. in Telecommunication Engineering from the University of Roma Tor Vergata (Italy) in 2006 and 2009, respectively and the Ph.D degree in Electrical and Computer Engineering from Georgia Tech, Atlanta, GA (USA) in January 2017. He was a Fulbright scholar at Georgia Tech (2012 - 2016) and a post-doctoral researcher at both the Sant’Anna School of Advanced Studies of Pisa (Italy, 2017 - 2018) and at the University of Roma Tor Vergata (Italy, 2019 - 2020). His research interests include wireless radio communications, microwave circuits, and mmWave antenna design.

Alessandro Di Carlofelice graduated in Electronic Engineering at the University of L’Aquila, in 2006, and earned a Ph.D in Microwave radiometry for remote sensing and bio-medical applications in 2011. In July 2006, he took part in the ESMO (European Student Moon Orbiter) program supported by ESA to design a microwave radiometer payload. Since February 2011, he has joined the Department of Electrical Engineering and Information, University of L’Aquila, as a Postdoctorate Researcher. His research activity is in the field of space systems for telecommunications, RFID and remote sensing.

Pietro Tognolatti graduated in Electronic Engineering at the University ”La Sapienza” of Rome, in 1981. From 1982 to 1984, he worked at the Research Division of Telespazio S.p.A. From 1984 to 1992, he was a researcher at the University of Rome Tor Vergata. He moved to the University of L’Aquila, as an Associate Professor in Microwaves, in 1992, and became Full Professor in 2000. From 2007 to 2012 he served as Head of the Electrical Engineering and Computer Science Department (DIEI) at the University of L’Aquila. His main scientific interests are medical application of microwaves, interactions between electromagnetic fields and human body, signal-processing, electromagnetic compatibility, and design of passive microwave circuits and antennas. His interests also include software defined radio issues and RFID systems.

Gaetano Marrocco Full Professor at the University of Roma Tor Vergata where he serves as chair of the Medical Engineering School. His research is currently focused on wireless-activated sensors, and, in particular, on Epidermal Electronics and structural antennas for smart prothesis, and finger augmentation devices for Tactile Internet. He is chair of the Italian Section of URSI Commission D Electronics and Photonics and of co-founder and president of the University spin-off RADIO6ENSE that is active in the short-range electromagnetic sensing for Industrial Internet of Things, Smart Manufacturing, Automotive and Digital Health.